1.E.1: 3.A

Nuclear Physics A321 (1979) 515–532; © *North-Holland Publishing Co., Amsterdam*

HIGH-SPIN YRAST LEVELS OF ^{38}Ar

H. J. M. AARTS, G. A. P. ENGELBERTINK, H. H. EGGENHUISEN † and L. P. EKSTRÖM ††

Fysisch Laboratorium, Rijksuniversiteit, Utrecht, The Netherlands

Received 27 October 1978

Abstract: High-spin states of ^{38}Ar have been studied with the ^{35}Cl(α, pγ)^{38}Ar reaction at E_α = 18 MeV and with the ^{24}Mg(^{16}O, 2pγ)^{38}Ar reaction at $E(^{16}O)$ = 38 and 45 MeV. The ^{38}Ar level scheme is obtained with the former reaction from a proton-γ coincidence measurement. Gamma-gamma coincidence, γ-ray angular distribution and linear polarization experiments have been performed with a Ge(Li)-Na(Tl) Compton suppression spectrometer and a three-crystal Ge(Li) Compton polarimeter. Unambiguous spin-parity assignments of $J^\pi = 7^-$, 7^+, 8^+, 7^-, 9^- and 11^- to the ^{38}Ar levels at E_x = 7.51, 8.08, 8.57, 8.97, 10.17 and 11.61 MeV, respectively, are obtained. The 8.57 MeV, 8^+ level has a mean life below 0.8 ps. Excitation energies, branching ratios, multipole mixing ratios and transition strengths are reported. The experimental results are compared with shell-model calculations.

E | NUCLEAR REACTIONS ^{35}Cl(α, pγ)^{38}Ar, E = 18 MeV; measured pγ-coin; ^{38}Ar deduced levels; ^{24}Mg(^{16}O, 2pγ)^{38}Ar, E = 38 and 45 MeV; measured $\sigma(E_\gamma, E)$, $\sigma(E, \theta)$, $\gamma\gamma$-coin, γ-ray lin. polarization, Doppler pattern; ^{38}Ar deduced levels, $T_{1/2}$, γ-branching, J, π, δ, transition strengths. Enriched targer, HP Ge, Compton suppression spectrometer, three-crystal Ge(Li) Compton polarimeter.

1. Introduction

Experiments with heavy-ion fusion-evaporation (HIFE) reactions, in which the basic properties of the HIFE process are exploited, have shown that these reactions are very suitable for detailed nuclear structure investigations of low-lying yrast states of light nuclei. High-spin levels in ^{38}Ar have been studied previously with the ^{27}Al(^{14}N, 2pnγ)^{38}Ar reaction [1]) and the ^{24}Mg(^{16}O, 2pγ)^{38}Ar reaction [2]), both at bombarding energies of about 40 MeV.

The ^{35}Cl(α, pγ)^{38}Ar reaction at E_α = 14 MeV has been used [3]) in an extensive investigation of ^{38}Ar levels up to 10 MeV excitation energy. From this work it became clear that in the HIFE studies mentioned above the measurement of γ-ray energies, intensities, (apparent) lifetimes and coincidence relations was not sufficient for the construction of the decay scheme in a unique way. Generally, arguments concerning the time order of γ-rays, which are based on intensity or

† Present address: Philips Research Laboratories, Eindhoven, The Netherlands.
†† Present address: Oliver Lodge Laboratory, Liverpool, Great Britain.

apparent lifetime considerations, are not correct if in the decay branches of appreciable intensity are missed. Errors in that respect have been made in refs. [1,2]), which were corrected in ref. [4]) on the basis of the results of ref. [3]).

The present work reports on work with the ^{24}Mg(^{16}O, 2pγ)^{38}Ar reaction at $E(^{16}O) = 38$ and 45 MeV and with the ^{35}Cl(α, pγ)^{38}Ar reaction at $E_\alpha = 18$ MeV to excite levels of higher spin than in ref. [3]). Globally, the (α, pγ) reaction serves to establish the level scheme and the heavy-ion reaction provides the definite spin-parity assignments which are lacking in the previous work [3,4]). States with spins up to $J = 11$ are excited in *both* reactions.

2. Experimental methods and analysis

Targets of about 300 μg/cm^2 ^{24}Mg, enriched to 99.94 %, on 30 μm Au backings were bombarded with 38 and 45 MeV $^{16}O^{6+}$ beams of 50–300 nA (electrical) from the Utrecht EN tandem accelerator. The position of the beam spot was defined by a 2.0 mm diameter Ta collimator, 25 mm in front of the target. At these bombarding energies high-spin states of ^{38}Ar are well populated as known from previous work [2]) and as expected from the grazing-collision picture shown in fig. 1. Fig. 2 gives the excitation function for the 493, 1201 and 1440 keV γ-rays, which stem from the decay of the lowest $J^\pi = 8^+$, 9^- and 11^- levels, respectively (see

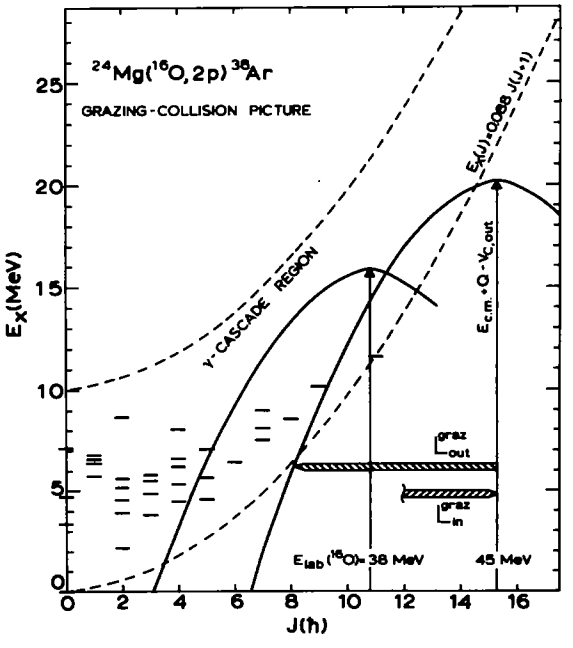

Fig. 1. The grazing collision picture for the ^{24}Mg(^{16}O, 2pγ)^{38}Ar reaction at bombarding energies of 38 and 45 MeV.

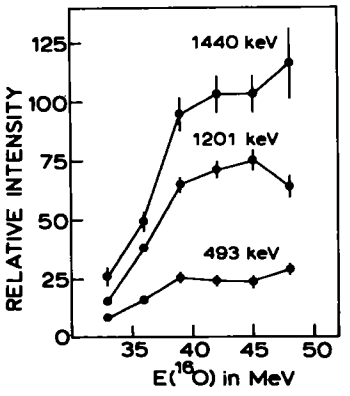

Fig. 2. The excitation function for the 493, 1201 and 1440 keV γ-rays, which appear in the decay of the lowest $J^{\pi} = 8^+$, 9^- and 11^- levels, respectively; see sect. 3.

sect. 3). The bombarding energy of 45 MeV was chosen on the basis of this result.

The γ-γ coincidence, γ-ray angular distribution and linear polarization measurements with the ^{24}Mg(^{16}O, 2pγ)^{38}Ar reaction are discussed below. The method of analysis, as summarized in subsect. 2.4, is identical to that of ref. [5-7]).

In addition a p-γ coincidence experiment with the ^{35}Cl(α, pγ)^{38}Ar reaction at $E_{\alpha} = 18$ MeV was performed with a target of 200 μg/cm^2 $BaCl_2$, enriched to 99 % in ^{35}Cl, on a carbon backing of 10 μg/cm^2.

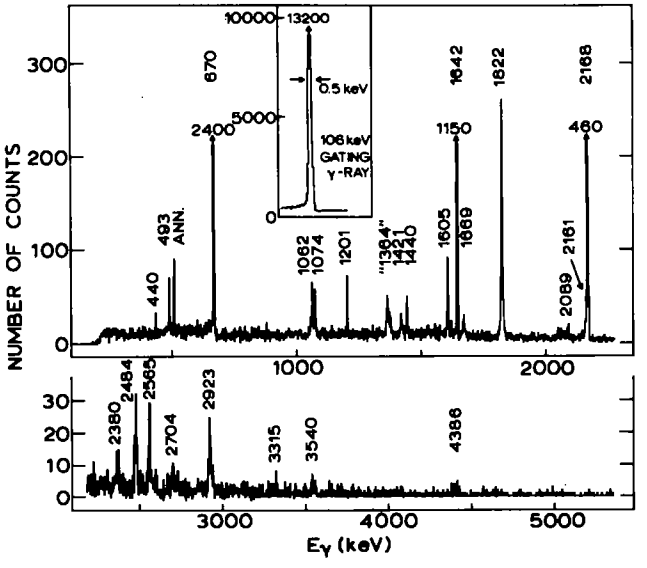

Fig. 3. The γ-ray spectrum from the CSS at $\theta_{\gamma} = 90°$, in coincidence with the 106 keV γ-ray in a 0.5 cm^3 HP Ge at a bombarding energy of $E(^{16}O) = 45$ MeV. The height of the 670, 1642 and 2168 keV peaks is given by the number above the arrow. The insert shows the gating γ-ray with its (low) background.

2.1. GAMMA-GAMMA COINCIDENCE MEASUREMENTS

The lowest $J^\pi = 5^-$ level at 4.59 MeV, which 90 % decays with a 106 keV γ-ray, is strongly fed in the decay of the high-spin states. Therefore a γ-γ coincidence experiment was performed with a 0.5 cm^3 HP Ge low-energy photon spectrometer (LEPS) at $\theta_\gamma = +90°$ and a large-volume Ge(Li)-NaI(Tl) Compton suppression spectrometer (CSS) at $\theta_\gamma = -90°$.

The coincidence events ($E_{+90°}$, $E_{-90°}$, Δt) are stored on magnetic tape for later off-line analysis. The advantage of using a LEPS is the relatively low background for a 106 keV gating γ-ray, which yields a more reliable coincidence spectrum (see fig. 3). The contributions from background and randoms are subtracted in the analysis.

In a similar way the CSS is combined with a large Ge(Li) detector for coincidences with γ-rays of higher energy.

2.2. ANGULAR DISTRIBUTION AND LINEAR POLARIZATION MEASUREMENTS

Angular distributions were measured with the CSS and a 24 % efficient Ge(Li) detector. The latter was shielded with 3 mm Pb and was used for the weaker high-energy γ-rays, such as $E_\gamma = 4386$ keV. Singles spectra were taken at six angles between $\theta_\gamma = 0°$ and 90°, evenly spaced in $\cos^2\theta_\gamma$. The angular distribution attenuation coefficients are calculated with the program of Krane [8]). The eccentricity of the set-up was measured with 1 mm diameter ^{133}Ba and ^{60}Co sources mounted at the position of the beam spot. The corrections, measured with an accuracy of 0.2 %, are less than 0.6 %.

Another Ge(Li) detector at $\theta_\gamma = -110°$ served as a monitor. The reaction-rate-dependent pulser technique is used to measure the relative dead-time losses of the monitor and moving detection systems.

Relative efficiencies are determined with ^{56}Co, ^{133}Ba and ^{226}Ra sources [9,10]) mounted at the position of the beam spot.

Gamma-ray linear polarizations are measured with a three-crystal Ge(Li) Compton polarimeter, as described in detail in ref. [5]). The relative efficiency of the two scatterer-absorber systems is measured with unpolarized γ-rays from several sources. The sensitivity of the polarimeter is determined from γ-rays of known polarization produced in (p, p'γ) and (p, nγ) reactions. In the off-line analysis single Compton-scattering events are selected to reduce the background.

2.3. PROTON-γ COINCIDENCE MEASUREMENT

In order to establish the ^{38}Ar level scheme, a p-γ coincidence experiment was performed with the ^{35}Cl(α, pγ)^{38}Ar reaction. Coincidences were recorded between a 24 % efficient Ge(Li) detector at $\theta_\gamma = 90°$ and a 1 mm thick annular Si counter

around $\theta_p = 180°$. The Si detector was shielded for scattered α-particles with 50 μm mylar. The coincident events (E_p, E_γ, Δt) were stored on magnetic tape for later off-line analysis. The contributions from background and randoms in the gates are subtracted in the analysis.

2.4. ANALYSIS OF J^π HYPOTHESES

The experimental information on transition strengths, as condensed in a set of recommended upper limits (RUL's) [11]), is used to restrict the J^π possibilities and the range of multipole mixing ratios to be investigated.

The angular distribution and linear polarization data are analysed without assumptions about the shape of the magnetic substate distribution, apart from the restriction that the spin alignment attenuation factor α_2 is positive in heavy-particle induced fusion evaporation reactions [12]). No limitations are imposed on α_4. In the mathematical treatment, the above mentioned restrictions are taken as rigorous. In the χ^2 analyses, a 99.9 % confidence limit is exercised in the investigation of the J^π hypotheses.

For the multipole mixing ratios the sign convention of Rose and Brink [13]) is used; the errors are determined according to ref. [14]).

3. Results

3.1. DECAY SCHEME

The γ-ray spectrum from the CSS at $\theta_\gamma = 90°$, in coincidence with the 106 keV γ-ray in the HP Ge detector, is displayed in fig. 3. The Compton background under the gating γ-ray of about 3 % of the peak height has been taken into account. Gamma-ray energies obtained from this spectrum are listed in table 1. The spectrum is calibrated internally. The peak labeled "1364" appears to be a doublet as discussed below. The 2161 and 2168 keV peaks are well resolved in the HP Ge singles spectrum of fig. 4. The 4386 keV γ-ray, weakly visible in fig. 3, shows up clearly in the Compton-suppressed singles spectrum of γ-rays of higher energy in fig. 5. The weak γ-rays at 2380, 2704 and 3540 keV could not be placed in the decay scheme.

The level scheme is obtained from a p-γ coincidence measurement with the ^{35}Cl(α, pγ)^{38}Ar reaction at $E_\alpha = 18$ MeV. Fig. 6 shows proton spectra in coincidence with particular γ-rays. Coincident proton spectra are generated for those γ-rays which appear in the decay of the high-spin states excited in the heavy-ion reaction (see fig. 3). The energies of these γ-rays observed in the (α, pγ) reaction agree to within 1 keV with those observed in the heavy-ion reaction. In order to populate the high-spin states of interest, the α-particle bombarding energy should be sufficiently high, which has, however, the disadvantage of populating a very large number of levels in a rather unselective manner.

TABLE 1

Energies of γ-rays observed in the $^{24}Mg(^{16}O, 2p\gamma)^{38}Ar$ reaction in coincidence with the 4586 → 4480 keV transition

E_γ (keV)	Assignment (E_x in ^{38}Ar in keV)	E_γ (keV)	Assignment (E_x in ^{38}Ar in keV)
492.7 ±0.2	8569 → 8078	1822.39±0.16 [a,c]	6408 → 4586
669.86±0.15 [a,b]	4480 → 3810	2088.6 ±0.3	6675 → 4586
1061.5 ±0.2	8569 → 7509	2160.5 ±0.2 [d]	8569 → 6408
1072.5 ±0.4	5658 → 4586	2167.53±0.05 [a,b]	2168 → 0
1201.4 ±0.2	10174 → 8973	2483.9 ±0.4	7070 → 4586
1364 ±4	9933 → 8569	2564.7 ±0.4	8973 → 6408
1364 ±4	11297 → 9933	2923.2 ±0.4	7509 → 4586
1420.8 ±0.3	8491 → 7070	3162.46±0.10 [a,b]	
1440.0 ±0.2	11614 → 10174	4386.2 ±0.4 [f]	8973 → 4586
1604.68±0.11 [a,c]	10174 → 8569		
1642.44±0.10 [a,b]	3810 → 2168		
1669.2 ±0.3	8078 → 6408		

[a]) Used for internal calibration.
[b]) Value taken from ref. [16]).
[c]) Value taken from ref. [2]).
[d]) From the LEPS spectrum of fig. 4.
[e]) From ^{35}Cl; peak position taken from the random spectrum.
[f]) From a singles spectrum.

The most energetic proton group in each coincident spectrum of fig. 6 is labeled with the corresponding excitation energy in ^{38}Ar and in the further analysis it is assumed that the gating γ-ray deexcites a level at this energy. The calibration of the proton detector is obtained from a similar run at the lower bombarding energy of $E_\alpha = 12$ MeV with the low-lying levels at 3.81, 4.48, 4.59, 5.66 and 6.41 MeV as calibration points.

Coincident with the 1440 keV γ-ray, a broad peak at an energy of 10.2 MeV is observed in addition to the $E_x = 11.61$ MeV peak. It appears to correspond to the (α, α_1) reaction on the ^{138}Ba content of the $BaCl_2$ target. The first excited state of ^{138}Ba has an excitation energy of 1436 keV [ref. [15])]. Coincident with the $E_\gamma = 1364 \pm 4$ keV doublet, proton peaks corresponding to $E_x = 11.29$ and 9.93 MeV, with a difference of 1.36 MeV are observed. They imply a 11.29 → 9.93 → 8.57 MeV cascade.

Combination of the data of fig. 6 with the γ-ray energies of table 1 results in the assignments of table 1 and the excitation energies of table 2. For comparison, results of refs. [1,4]) and ref. [3]) are given in columns 2 and 3, respectively. The present available information on lifetimes for these states is collected in column 4 of table 2. The present τ_m limit for the 8.57 MeV level is detailed in subsect. 3.2.2.

The above results in combination with γ-γ coincidence data from the $^{24}Mg(^{16}O, 2p)^{38}Ar$ reaction lead to the decay scheme of fig. 7. The branching ratios

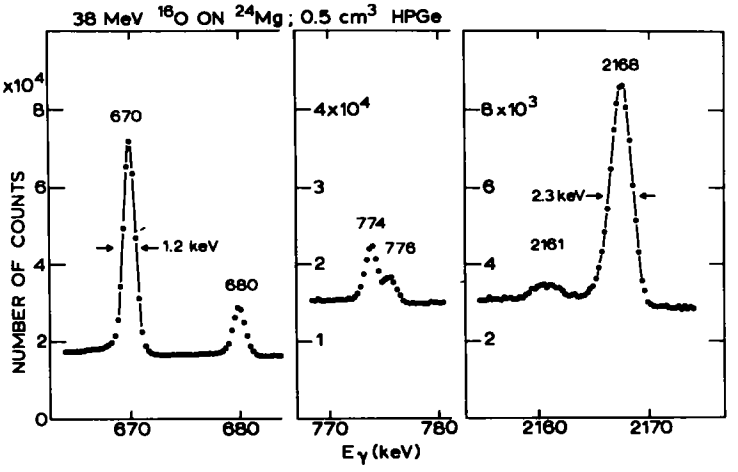

Fig. 4. Some doublets as observed with the HP Ge detector in singles. The doublet consisting of 774 keV [^{38}K(3420 → 2646 keV)] and 776 keV [^{38}Ar(4586 → 3810 keV)] may be responsible for the confusion in ref. [1]) about the branching of the ^{38}Ar, 4586 keV level.

for the 8.57, 8.97 and 10.17 MeV levels follow from the γ-ray intensities obtained in the angular distribution measurements.

3.2. SPIN-PARITY ASSIGNMENTS

A linear polarization spectrum from ^{24}Mg+^{16}O at $E(^{16}\text{O}) = 38$ MeV is shown in fig. 8. The ratio of peak areas from the difference and sum spectra corresponds to the experimental assymmetry $A = (aN_\perp - N_\parallel)/(aN_\perp + N_\parallel)$; see ref. [5]). The

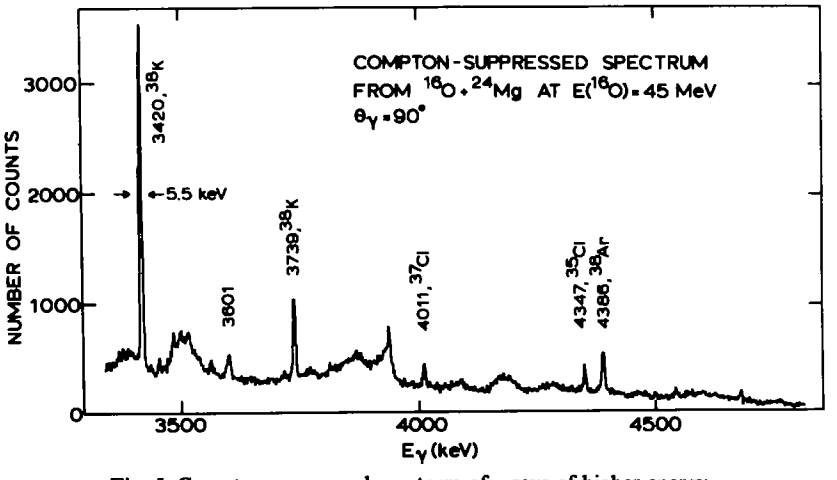

Fig. 5. Compton suppressed spectrum of γ-rays of higher energy.

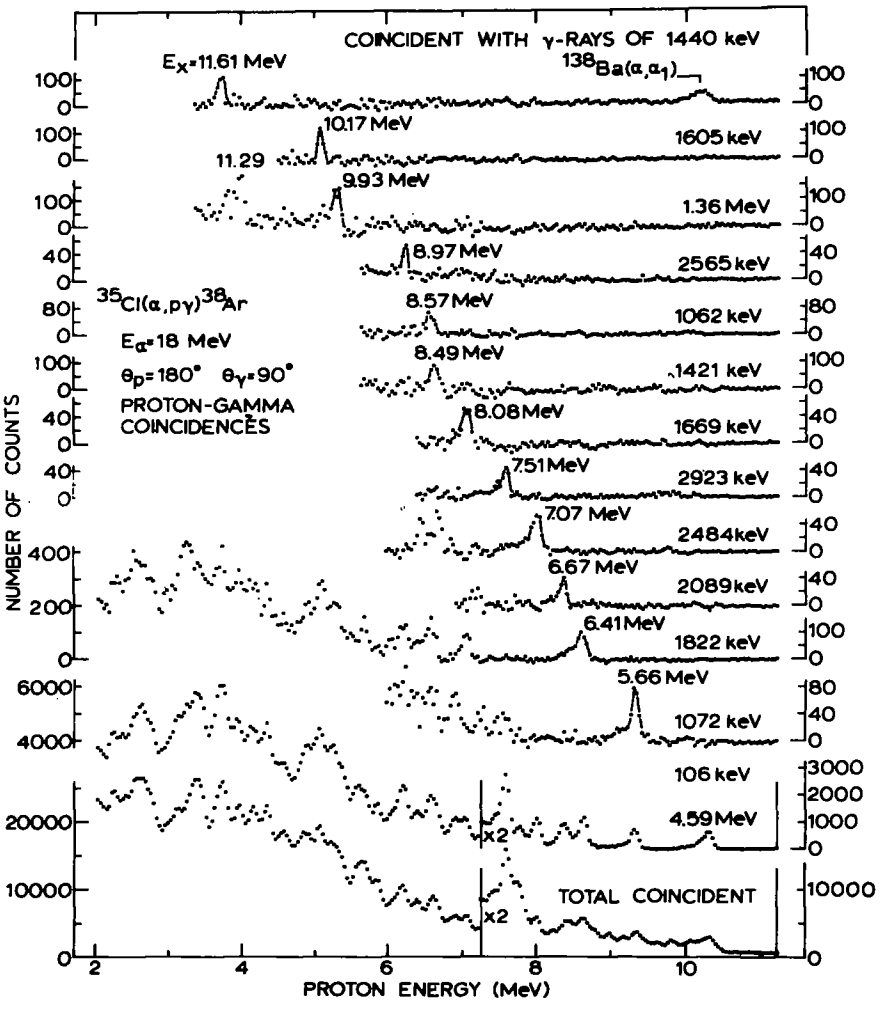

Fig. 6. Proton groups of the $^{35}Cl(\alpha, p)^{38}Ar$ reaction in coincidence with particular γ-rays. The most energetic group in each coincident proton spectrum is labeled with the corresponding excitation energy in ^{38}Ar.

measured linear polarizations are given in column 6 of table 3. Columns 4 and 5 of this table list the angular distribution coefficients of the relevant transitions. The results are summarized in table 4.

3.2.1. The E_x = 8.97 MeV level. This level decays with $\tau_m < 40$ fs [ref. [3])] and branching ratios of $(31 \pm 5)\%$, $(8 \pm 2)\%$ and $(61 \pm 5)\%$ to the E_x = 4.59, 5.66 and 6.41 MeV levels with $J^\pi = 5^-$, 5^- and 6^+, respectively. The mean life and decay in combination with the RUL's of ref. [11]) exclude for the 8.97 → 6.41 MeV transition pure octupole and M2 character and limit the E1/M2 mixing ratio to

TABLE 2

Excitation energies and mean lives of high-spin states in ^{38}Ar

E_x (keV)			τ_m (ps)
[a]	[b]	[c]	
6408.3±0.2 [d]	6408.1±0.3	6408±1	1.5 ±0.4 [d]
6674.5±0.4		6674±1	
7069.9±0.4		7070±2	0.074±0.020 [c]
7509.2±0.4	7507.7±0.3	7507±1	0.06 < τ_m < 2 [b,c]
8077.5±0.4	8076.6±0.4	8077±2	0.16 ±0.04 [c]
8490.7±0.5		8488±2	
8569.4±0.3	8569.1±0.3	8568±2	< 0.8 ps [a]
8972.5±0.5	8972.2±0.5	8972±1	≦ 0.04 [c]
9933 ±4		9928±2	
10174.2±0.4	10173.5±0.4		6 ±2 [b]
11297 ±6			
11614.2±0.5	11613.8±0.5		7 ±3 [b]

[a]) Present work. [b]) Refs. [1,4]). [c]) Ref. [3]). [d]) Ref. [2]).

$|\delta_{2.56}| < 0.074$. Pure octupole and M2 character is similarly excluded for the 8.97 → 4.59 MeV transition, so that mean life, decay and RUL's limit the spin-parity possibilities to J^π(8.97 MeV) = 4^+, $5^\pm$, $6^\pm$ or 7^-. Fig. 9 gives the angular distributions for the 2565 and 4386 keV transitions.

The result of a combined analysis of the angular distributions and polarizations of the 8.97 → 6.41 and 8.97 → 4.59 MeV transitions for the above J^π hypotheses is shown in fig. 10. For each J^π hypothesis, the χ^2 per degree of freedom is displayed as a function of $\delta_{4.39}$ while minimized with respect to α_2, α_4 and $\delta_{2.56}$. The values of

TABLE 3

Gamma-ray angular distribution and linear polarization results obtained in the ^{24}Mg(^{16}O, 2pγ)^{38}Ar reaction

E_{x1} (keV)	E_γ (keV)	Rel. intensity	100 A_2	100 A_4	100 P
6408	1822	1000±30	−30± 2	− 1± 2	+40± 5
7509	2923	150± 9	+57± 7	−59± 8	+68±11
8569	2161	130± 9	+56±25 [a])	−39±20 [a])	+66±22
	1062	28± 7			
	493	28± 5	− 8±40		−56± 8
8973	4387	86±14	+43± 5	−21± 5	+65±44
	3315	22± 6			
	2565	169±14	−30± 6	− 2± 8	+57±13
10174	1605	187± 7	−20± 6	+ 1± 6	+40± 6
	1201	173± 7	+40± 3	−18± 3	+64± 6
11614	1440	140± 5	+38± 3	−20± 3	+57± 8

[a]) From ref. [2]).

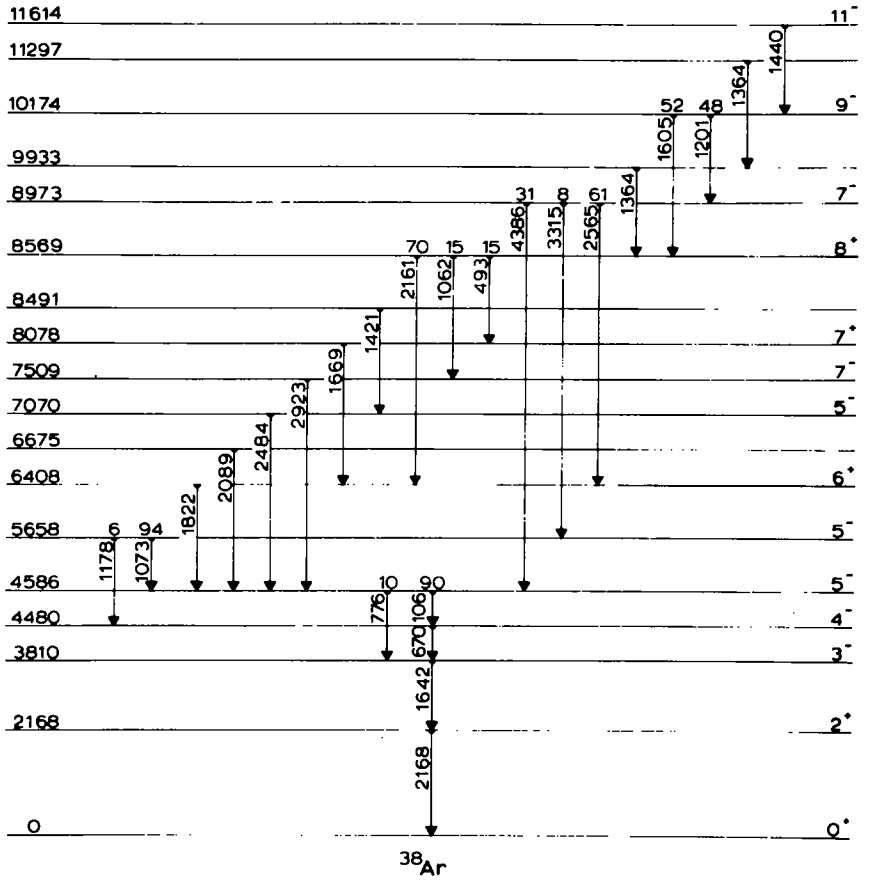

Fig. 7. Partial decay scheme of ^{38}Ar.

the spin alignment attenuation factors α_2, α_4 and the mixing ratio $\delta_{2.56}$ are restricted as follows: (i) $\alpha_2 \geqq 0$, (ii) α_4 free, (iii) $|\delta_{2.56}| < \infty$, < 0.074 or < 0.8 for M1/E2, E1/M2 and E2/M3 mixtures, respectively.

The analysis yield J^{π}(8.97 MeV) = 7^-, α_2(8.97 MeV) = 1.0 ± 0.1, α_4(8.97 MeV) = 1.0 ± 0.2 and $\delta_{2.56} = +0.04\pm0.02$. The M3 RUL of 10 W.u. leads to $|\delta_{4.39}| < 0.007$. The 8.97 → 4.59 MeV, $7^- \rightarrow 5^-$ transition has an E2 strength of > 0.5 W.u. and the 8.97 → 6.41 MeV, $7^- \rightarrow 6^+$ transition an E1 strength of > 0.8 m.W.u.

3.2.2. The E_x = 10.17 and 8.57 MeV levels. The 10.17 MeV level decays with $\tau_m = 6\pm2$ ps [ref. [4])] and branching ratios of $(52\pm2)\%$ and $(48\pm2)\%$ to the E_x = 8.57 and 8.97 MeV levels, respectively. The mean life and decay in combination with the RUL's exclude for the 10.17 → 8.97 MeV transition pure octupole

TABLE 4

Strengths of transitions between ^{38}Ar levels of high spin

$E_{xi} \rightarrow E_{xf}$ (MeV)	E_γ (keV)	$J_i^\pi \rightarrow J_f^\pi$	Branching (%)	100 δ	Transition strength (W.u.)
7.51 → 4.59	2923	$7^- \rightarrow 5^-$	100		E2: 0.3–8
→ 5.66	1851	$7^- \rightarrow 5^-$	< 4		
8.08 → 6.41	1669	$7^+ \rightarrow 6^+$	100		M1: 0.04 ± 0.01 [a])
8.57 → 6.41	2161	$8^+ \rightarrow 6^+$	70 ± 4		E2: > 2
→ 7.51	1062	$8^+ \rightarrow 7^-$	15 ± 4		E1: $> 1.3 \times 10^{-4}$ [a])
→ 8.08	493	$8^+ \rightarrow 7^+$	15 ± 3	< +9	M1: > 0.05
8.97 → 4.59	4387	$7^- \rightarrow 5^-$	31 ± 5		E2: > 0.5
→ 5.66	3315	$7^- \rightarrow 5^-$	8 ± 2		E2: > 0.5
→ 6.41	2565	$7^- \rightarrow 6^+$	61 ± 5	$+4 \pm 2$	E1: $> 8 \times 10^{-4}$
10.17 → 7.51		$9^- \rightarrow 7^-$	< 5		E2: < 0.007
→ 8.57	1605	$9^- \rightarrow 8^+$	52 ± 2	-4 ± 2	E1: $(1.8 \pm 0.6) \times 10^{-5}$
→ 8.97	1201	$9^- \rightarrow 7^-$	48 ± 2		E2: 3.5 ± 1.2
11.61 → 10.17	1440	$11^- \rightarrow 9^-$	100		E2: 2.5 ± 1.0

[a]) Calculated under the assumption that the mixing ratio is zero.

and M2 character and limit the spin-parity possibilities to $J^\pi(10.17\ \text{MeV}) = 5^-, 6^\pm, 7^\pm, 8^\pm$ or 9^-.

Analysis of the angular distribution and polarization of the 10.17 → 8.97 MeV transition yields $J^\pi(10.17\ \text{MeV}) = 9^-$. The χ^2 analysis is carried out under the restrictions (i) $\alpha_2 > 0$, (ii) α_4 free, (iii) $|\delta_{1.20}| < \infty$ for dipole/quadrupole and $|\delta_{1.20}| < 0.1$ for E2/M3 mixtures.

The M3 RUL leads to $|\delta_{1.20}| < 0.001$ and the 10.17 → 8.97 MeV, $9^- \rightarrow 7^-$ transition has an E2 strength of 3.5 ± 1.2 W.u.

The 8.57 MeV level decays by 2161, 1062 and 493 keV γ-rays with branching ratios of $(70 \pm 4)\%$, $(15 \pm 4)\%$ and $(15 \pm 3)\%$, respectively. The lifetime limit for this level is obtained from the Doppler patterns of the 493 keV γ-ray. The patterns of fig. 11 are taken with the CSS in singles at angles between $\theta_\gamma = 75°$ and 115° and with a target of 470 μg/cm^2 ^{24}Mg on 20 μm Au. The data show that the 493 keV peak, which is broadened at $\theta_\gamma = 90°$, consists of a stopped and a shifting component. The stopped component is due to feeding from the 6 ps, 10.17 MeV level, while the shifting component reflects the lifetime of the 8.57 MeV level itself in combination with lifetimes of other (relatively fast) feeding levels. Interpretation of the shifted part of the pattern results in an upper limit of 0.8 ps for τ_m(8.57 MeV). This limit restricts the 2161 keV (8.57 → 6.41 MeV) transition to dipole or electric quadrupole radiation. The 1605 keV 10.17 → 8.57 MeV transition is on the basis of its lifetime also restricted to dipole or electric quadrupole radiation. The feeding of the 8.57 MeV level from the 9^- level and its decay to the 6^+ level then limit the spin-parity possibilities to $J^\pi(8.57\ \text{MeV}) = 7^-$ or 8^+. The χ^2 analysis of the angular distribution and polarization of the 10.17 → 8.57 MeV transition then yields $J^\pi(8.57\ \text{MeV}) = 8^+$.

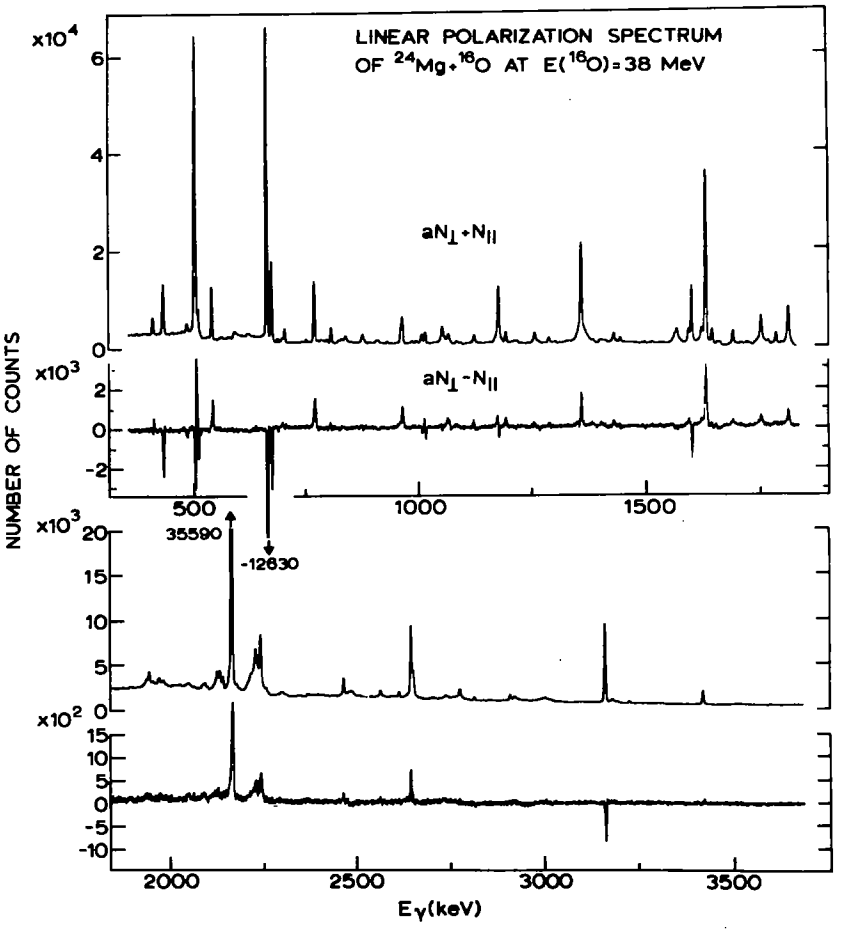

Fig. 8. Sum and difference spectra from the γ-ray linear polarization measurement.

The ensuing E2 strength of the 2161 keV (8.57 → 6.41 MeV, $8^+ \rightarrow 6^+$) transition is > 2.0 W.u. The mixing ratio of the 1605 keV (10.17 → 8.57 MeV, $9^- \rightarrow 8^+$) transition determined in a fit to the data for the 10.17 → 8.57 and 10.17 → 8.97 MeV transitions together is $\delta_{1605} = -0.04 \pm 0.02$.

3.2.3. The E_x = 11.61 MeV level. The 11.61 MeV level decays with $\tau_m = 7 \pm 3$ ps [ref. [1])] only to the 10.17 MeV level. The mean life and decay in combination with the RUL's exclude pure octupole and M2 character for this 1440 keV transition and limit the J^π possibilities to J^π(11.61 MeV) = 7^-, $8^\pm$, $9^\pm$, $10^\pm$ or 11^-.

Analysis of the angular distribution and polarization of the 11.61 → 10.17 MeV transition yields J^π(11.61 MeV) = 11^-. The χ^2 analysis, shown in fig. 12, is carried out under the restrictions (i) $\alpha_2 \geqq 0$, (ii) α_4 free, (iii) $|\delta_{1.44}| < \infty$ for M1/E2 and $|\delta_{1.44}| < 0.18$ for E1/M2 mixtures.

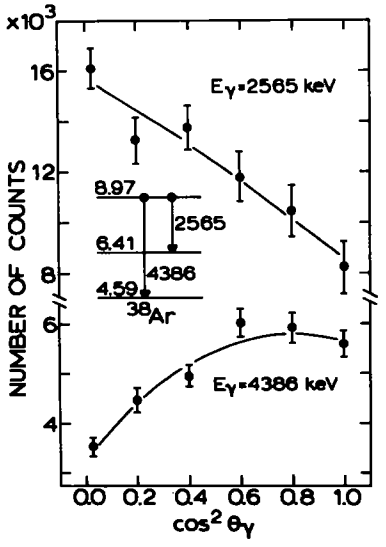

Fig. 9. Angular distributions for the 2565 and 4386 keV transitions.

The M3 RUL leads to $|\delta_{1.44}| < 0.001$ and the 11.61 → 10.17 MeV, $11^- \rightarrow 9^-$ transition has an E2 strength of 2.5 ± 1.0 W.u.

3.2.4. The E_x = 8.08 MeV level. The 8.08 MeV level is fed by a 493 keV transition from the 8.57 MeV, $J^\pi = 8^+$ level. The upper limit of τ_m(8.57 MeV) < 0.8 ps restricts this 493 keV transition to dipole radiation and thus limits the spin-parity possibilities for the 8.08 MeV level to J^π(8.08 MeV) = $7^\pm$, $8^\pm$ or $9^\pm$.

The 8.08 MeV level decays with $\tau_m = 160 \pm 40$ fs [ref. [3])] with a 1669 keV

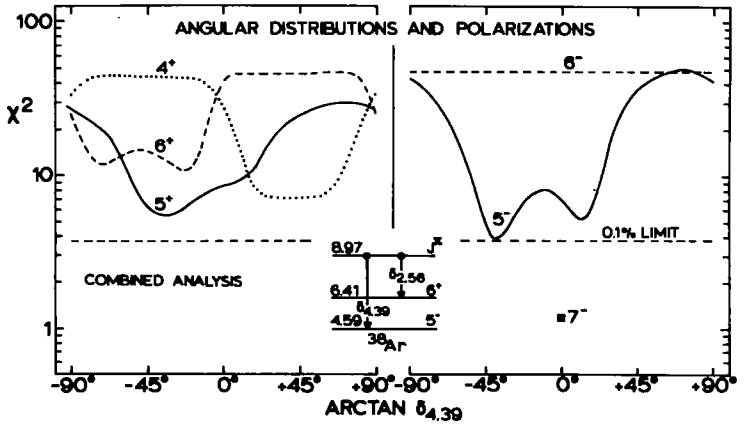

Fig. 10. Results of the least-squares analysis of the combined angular distribution and polarization data for the 2565 and 4386 keV transitions (see subsect. 3.2.1).

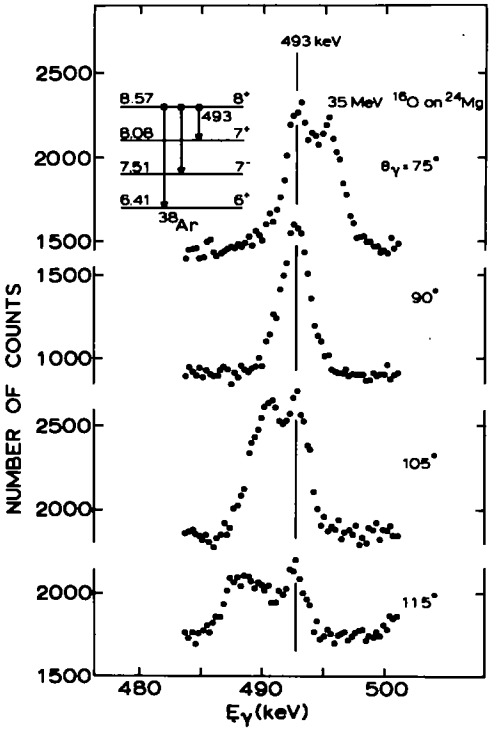

Fig. 11. Doppler patterns of the 493 keV γ-ray observed with the CSS in singles. Interpretation of the shifting part leads to an upper limit of 0.8 ps for τ_m (8.57 MeV).

transition to the 6.41 MeV, $J^\pi = 6^+$ level. This lifetime eliminates octupole or M2 character for the 1669 keV transition, such that J^π(8.08 MeV) = $7^\pm$ or $8^\pm$.

Analysis of the angular distribution and polarization of the 8.57 → 8.08 MeV transition yields J^π(8.08 MeV) = 7^+ and δ(8.57 → 8.08 MeV) < +0.09. The J^π(8.08 MeV) = $(5, 7)^+$ result given in ref. [3]) supports the present assignment.

3.2.5. The E_x = 7.51 MeV level. The 7.51 MeV level has a mean life of $\tau_m = 0.06-2$ ps [refs. [1, 3])] and decays with a 2923 keV transition to the 4.59 MeV, $J^\pi = 5^-$ level. The level is fed by a 1062 keV transition from the 8.57 MeV, $J^\pi = 8^+$ level. The lifetimes involved exclude pure M2 or octupole radiation for the 1062 and 2923 keV transitions and thus lead to J^π(7.51 MeV) = 6^+ or 7^-. The present data do not allow to distinguish between these two possibilities.

In ref. [3]) the assignment J(7.51) = 5 or 7 was obtained. Combination of both results gives J^π(7.51 MeV) = 7^-. The E2 strength of the 7.51 → 4.59 MeV, $7_1^- \rightarrow 5_1^-$ transition is between 0.3 and 8 W.u.

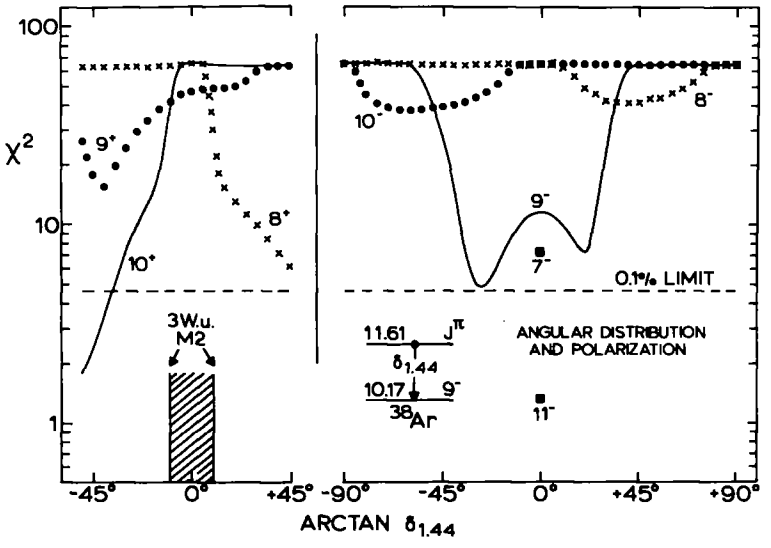

Fig. 12. Results of the least-squares analysis of the angular distribution and polarization data of the 1440 keV transition of ^{38}Ar (see subsect. 3.2.3).

4. Discussion

The data in fig. 6 show that the 2.56 MeV transition should be placed between the 8.97 and 6.41 MeV levels. The order of the two γ-rays in the $10.17 \xrightarrow{2.56} 7.61 \xrightarrow{1.20} 6.41$ cascade (excitation and γ-ray energies in MeV) as given in refs. [1,2]) is therefore incorrect. The cascade should be $10.17 \xrightarrow{1.20} 8.97 \xrightarrow{2.56} 6.41$. The data of fig. 6 further show that the 1.60 MeV transition deexcites the 10.17 MeV level. The cascade $10.17 \xrightarrow{2.16} 8.01 \xrightarrow{1.60} 6.41$ MeV given in ref. [2]) should therefore be reordered in $10.17 \xrightarrow{1.60} 8.57 \xrightarrow{2.16} 6.41$ MeV. The arguments concerning the time order of γ-rays which were used in refs. [1,2]) are based on intensity [1]) or apparent lifetime [2]) considerations. Such arguments fail if in the decay branches of appreciable intensity (e.g. the 3.32 and 4.38 MeV transitions from the 8.97 MeV level) are missed, by which the amount of sidefeeding of a level is deduced incorrectly. Particle spectroscopy is then needed to resolve such problems.

The present results agree with the corrections deduced by Warburton *et al.* [4]) from the particle-γ coincidence results of Glatz *et al.* [3]). In ref. [3]) the ^{35}Cl(α, pγ)^{38}Ar reaction is extensively studied at $E_\alpha = 14$ MeV. The γ-decay of 93 levels between 6.8 and 10 MeV excitation energy has been measured and the high-spin levels at 7.51, 8.08, 8.57 and 8.97 MeV are observed.

In the present ^{35}Cl(α, pγ)^{38}Ar experiment at $E_\alpha = 18$ MeV the $J^\pi = 9^-$ and 11^- states at 10.17 and 11.61 MeV (see fig. 6) are excited in addition. The grazing angular momentum for this α-particle bombarding energy amounts to $L_{in}^{graz} \approx 9$.

The mean lives of table 2 and the spins, branching ratios and mixing ratios in

table 4 lead to the transition strengths given in the last column of table 4. The 9^- level at 10.17 MeV decays to the 7^- level at 8.97 MeV, but not to the lower-lying 7^- level at 7.51 MeV. The latter E2 transition is weaker by more than a factor of 500. The E2 transitions between the high-spin levels have strengths of a few W.u. and indicate a predominantly single-particle character for these states.

The situation is not very encouraging as far as large-basis shell-model calculations are concerned. An appropriate shell-model space would require the inclusion of holes in the $1d_{\frac{3}{2}}$ shell but the dimensions of the matrices to diagonalize are then too large to handle [17]). Two unpublished calculations [18, 19]), performed in a smaller space, are, however, available for comparison with experiment.

The first calculation (named TH 1) has been carried out by Hasper [18]) with an effective interaction in a $(2s_{\frac{1}{2}}, 1d_{\frac{3}{2}})^{10-n}(1f_{\frac{7}{2}}, 2p_{\frac{3}{2}})^n$ configuration space ($n = 0$ or 2) for positive parity states. The negative parity states are calculated in a $(2s_{\frac{1}{2}}, 1d_{\frac{3}{2}}, 1f_{\frac{7}{2}},$

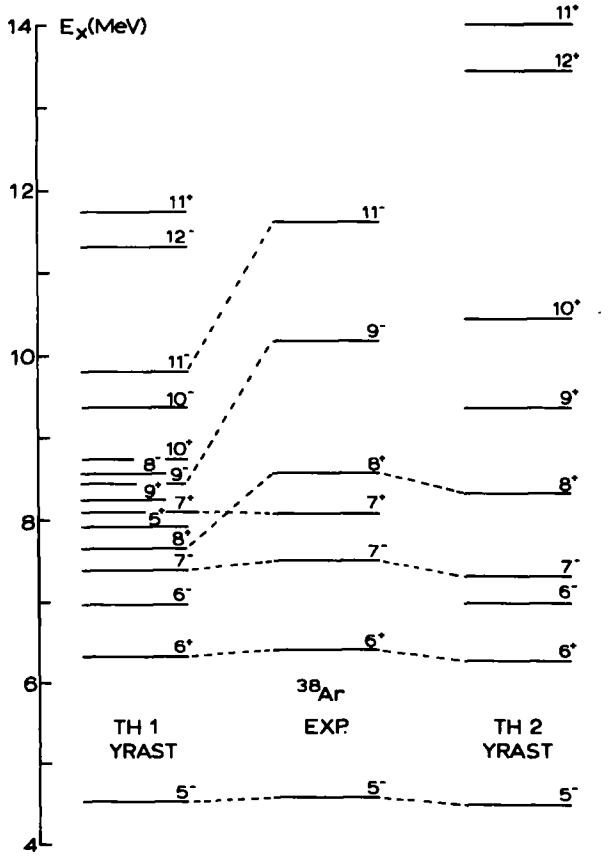

Fig. 13. Comparison of two theoretical calculations of the ^{38}Ar spectrum of yrast levels with experimental results.

$2p_{\frac{1}{2}})^{10}$ space with the restrictions: $n(2s_{\frac{1}{2}}) \geqq 2$, $n(1f_{\frac{7}{2}}) \leqq 3$ and $n(2p_{\frac{3}{2}}) \leqq 1$. The parameters of the interaction are obtained in a least-squares fit to experimentally well-established states in the $A = 35$–40 mass region. The resulting yrast spectrum is shown in fig. 13.

The second (more restricted) calculation (named TH 2) is from Wildenthal [19]) and is discussed in ref. [1]) (see especially table V of that reference). The calculated yrast spectrum is also compared to the experimental results in fig. 13.

Fig. 13 shows that up to $J = 7$ the calculations TH 1 and TH 2 agree well with each other and with the experimental results. For $J \geqq 8$, however, the TH 1 energy scale seems compressed relative to TH 2. In TH 1, the $J^\pi = 10^+$ and 11^+ yrast states e.g. are predicted lower by 1.7 and 2.2 MeV, respectively. Unfortunately, predictions for the $J^\pi = 9_1^-$ and 11_1^- levels are not given in TH 2. They can, however, be estimated from TH 1 if it is assumed that in both calculations the energy differences with respect to the 10_1^+ level are the same. This would then lead to $E_x(9_1^-) = 10.1$ MeV and $E_x(11_1^-) = 11.5$ MeV, very close to the experimental 9^- and 11^- levels at 10.17 and 11.61 MeV, respectively.

The above consideration and the tendency of HIFE reactions to populate predominantly yrast levels make it likely that the investigated $J^\pi = 8^+, 9^-$ and 11^- levels at $E_x = 8.57$, 10.17 and 11.61 MeV, respectively, are indeed yrast.

The excitation energy of the lowest $J^\pi = 6^-$ level is experimentally not known [16]) Both theoretical calculations predict $E_x(6_1^-) = 6.98$ MeV. Ref. [18]) predicts in addition that it predominantly decays to the 5_1^- level. If we assume that the 6_1^- level is excited in the ^{24}Mg + ^{16}O reaction then a γ-ray of about 2.39 MeV should show up in the coincidence spectrum of fig. 3. It is possible that the 2380.5 ± 0.4 keV γ-ray in fig. 3, which is not placed in the level scheme, directly feeds the 4.59 MeV level. This would then lead to a level at $E_x = 6966.4 \pm 0.4$ keV.

One should, however, realize that (i) the intensity of the 2380 keV γ-ray in the p-γ coincidence experiment with the ^{35}Cl(α, pγ)^{38}Ar reaction is too weak to look for the corresponding proton group, (ii) refs. [3, 16]) report no levels at this excitation energy, (iii) angular distribution and polarization information for the 2380 keV γ-ray is absent due to its weak intensity in the heavy-ion reaction.

The assistance of D. E. C. Scherpenzeel and C. J. van der Poel in the last stages of the present investigation is much appreciated.

This work was performed as part of the research programme of the "Stichting voor Fundamenteel Onderzoek der Materie" (FOM) with financial support from the "Nederlandse Organisatie voor Zuiver-Wetenschappelijk Onderzoek" (ZWO).

References

1) J. J. Kolata *et al.*, Phys. Rev. **C13** (1976) 1944
2) M. A. van Driel *et al.*, Nucl. Phys. **A272** (1976) 466
3) F. Glatz *et al.*, Z. Phys. **A278** (1976) 319

4) E. K. Warburton, J. J. Kolata and J. W. Olness, Phys. Rev. **C16** (1977) 2075
5) H. H. Eggenhuisen *et al.*, Nucl. Phys. **A285** (1977) 167
6) H. H. Eggenhuisen *et al.*, Nucl. Phys. **A299** (1978) 175
7) H. H. Eggenhuisen *et al.*, Nucl. Phys. **A305** (1978) 245
8) K. S. Krane, Nucl. Instr. **98** (1972) 205; **109** (1973) 401
9) R. J. Gehrke, R. G. Helmer and R. C. Greenwood, Nucl. Instr. **147** (1977) 405
10) V. Zobel *et al.*, Nucl. Instr. **141** (1977) 329
11) P. M. Endt and C. van der Leun, Nucl. Phys. **A235** (1974) 27
12) G. A. P. Engelbertink *et al.*, Nucl. Instr. **143** (1977) 161;
G. A. P. Engelbertink, Proc. Conf. on physics of medium licht nuclei, Florence (1977) p. 256
13) H. J. Rose and D. M. Brink, Rev. Mod. Phys. **39** (1967) 306
14) A. N. James, P. J. Twin and P. A. Butler, Nucl. Instr. **115** (1974) 105
15) S. C. Pancholi and M. J. Martin, Nucl. Data Sheets **18** (1976) 167
16) P. M. Endt and C. van der Leun, Nucl. Phys. **A310** (1978) 1
17) H. Hasper (Groningen University), thesis 1974 and P. W. M. Glaudemans (Utrecht University), private communication
18) H. Hasper (Groningen University), Phys. Rev. C, submitted; and private communication
19) B. H. Wildenthal, unpublished, see ref. [1])